



# Sex- and APOE-specific genetic risk factors for late-onset Alzheimer's disease: Evidence from gene–gene interaction of longevity-related loci

Serena Dato<sup>1</sup> | Francesco De Rango<sup>1</sup> | Paolina Crocco<sup>1</sup> | Stefano Pallotti<sup>2</sup> | Michael E. Belloy<sup>3</sup> | Yann Le Guen<sup>3</sup> | Michael D. Greicius<sup>3</sup> | Giuseppe Passarino<sup>1</sup> | Giuseppina Rose<sup>1</sup> | Valerio Napolioni<sup>2</sup>

<sup>1</sup>Department of Biology, Ecology and Earth Sciences, University of Calabria, Rende, Italy

<sup>2</sup>Genomic And Molecular Epidemiology (GAME) Lab., School of Biosciences and Veterinary Medicine, University of Camerino, Camerino, Italy

<sup>3</sup>Department of Neurology and Neurological Sciences, School of Medicine, Stanford University, Stanford, California, USA

## Correspondence

Valerio Napolioni, School of Biosciences and Veterinary Medicine, University of Camerino, Via Gentile da Varano III, 62032 Camerino, Italy.  
Email: [valerio.napolioni@unicam.it](mailto:valerio.napolioni@unicam.it)

## Funding information

Alzheimer's Association, Grant/Award Number: AARF-20-683984; Italian Ministry of Education, University and Research, Grant/Award Number: PON ARS01\_00568; National Institutes of Health, Grant/Award Number: K99AG075238 and P30AG066515

## Abstract

Advanced age is the largest risk factor for late-onset Alzheimer's disease (LOAD), a disease in which susceptibility correlates to almost all hallmarks of aging. Shared genetic signatures between LOAD and longevity were frequently hypothesized, likely characterized by distinctive epistatic and pleiotropic interactions. Here, we applied a multidimensional reduction approach to detect gene–gene interactions affecting LOAD in a large dataset of genomic variants harbored by genes in the insulin/IGF1 signaling, DNA repair, and oxidative stress pathways, previously investigated in human longevity. The dataset was generated from a collection of publicly available Genome Wide Association Studies, comprising a total of 2,469 gene variants genotyped in 20,766 subjects of Northwestern European ancestry (11,038 LOAD cases and 9,728 controls). The stratified analysis according to APOE\*4 status and sex corroborated evidence that pathways leading to longevity also contribute to LOAD. Among the significantly interacting genes, *PTPN1*, *TXNRD1*, and *IGF1R* were already found enriched in gene–gene interactions affecting survival to old age. Furthermore, interacting variants associated with LOAD in a sex- and APOE-specific way. Indeed, while in APOE\*4 female carriers we found several inter-pathway interactions, no significant epistasis was found in APOE\*4 negative females; conversely, in males, significant intra- and inter-pathways epistasis emerged according to APOE\*4 status. These findings suggest that interactions of risk factors may drive different trajectories of cognitive aging. Beyond helping to disentangle the genetic architecture of LOAD, such knowledge may improve precision in predicting the risk of dementia and enable effective sex- and APOE-stratified preventive and therapeutic interventions for LOAD.

**Abbreviations:** AD, alzheimer's disease; APOE, apolipoprotein E; CV, cross-validation; GWAS, genome wide association study; IBD, identity-by-descent; IG, information gain; IGF1, insulin growth factor 1; LD, linkage disequilibrium; LOAD, late-onset alzheimer's disease; MAF, minor allele frequency; MDR, multifactor dimensionality reduction; QTL, quantitative trait locus; SNP, single nucleotide polymorphism.

Serena Dato and Francesco De Rango—Co-first authors.

Giuseppina Rose and Valerio Napolioni—Co-last authors.

This is an open access article under the terms of the [Creative Commons Attribution](https://creativecommons.org/licenses/by/4.0/) License, which permits use, distribution and reproduction in any medium, provided the original work is properly cited.

© 2023 The Authors. *Aging Cell* published by Anatomical Society and John Wiley & Sons Ltd.



## KEYWORDS

Alzheimer's Disease, epistasis, gene–gene interaction, IGF1, longevity, polymorphism

## 1 | INTRODUCTION

Alzheimer's disease (AD) is the most prevalent disease among people over 85 years of age in western countries, posing a significant challenge to public health systems around the world. Most AD cases are sporadic or late onset (LOAD; >65 years of age), with biological measures of disease being detectable as early as 20 years before the first cognitive symptoms are observed (Jagust, 2018). Decades of research have shed light on the neuropathological changes happening in the AD brain, and its complex etiology (Long & Holtzman, 2019), characterized by sex differences in several aspects of the disease, including its onset and progression, and the effects of *APOE*\*4 genotype, the strongest common genetic risk factor for LOAD (Nebel et al., 2018). A current challenge is to clarify the contribution of genetic, epigenetic, and environmental factors in the multifactorial nature of LOAD, which shows a heritability of 58%–79%, with a large fraction attributable to the *APOE* locus. Genetic studies over the last few years, particularly coming from genome-wide association studies (GWAS) and large sequencing projects, have changed the perception of LOAD, highlighting its polygenic nature with multiple susceptibility genetic loci (Andrews et al., 2023). Also, functional genomic analyses pointed out that common LOAD risk variants operate in complex networks of genetic and metabolic interactions, regulated by “hub” genes and “peripheral master regulators” (Gui et al., 2021). In the interactome network of the cell, each variant may show different effects (either in magnitude or in direction) on disease onset, in relation to alleles at other loci (Ridge et al., 2016). These epistatic effects may contribute substantially to the variation in disease susceptibility; that is, people carrying risk factors for LOAD but resilient to the disease, as well as people carrying the risk allele *APOE*\*4 who live into their 90s without developing dementia.

While advances in technologies and increased availability of multi-omics data have expanded our knowledge about LOAD genetic architecture, many risk variants remain to be identified (Andrews et al., 2023). Such variants may be found in the underlying processes leading to LOAD, such as inflammation (Akiyama et al., 2000), apoptosis (Behl, 2000), stress response (Iatrou et al., 2021), and mitochondrial decay (Kwong et al., 2006). Interestingly, many of these mechanisms are common to human longevity, suggesting that the search of susceptibility factors could be enhanced by testing genes belonging to pathways influencing longevity and survival. As a proof-of-concept alongside *APOE*, which is the locus consistently associated with longevity across different populations (Abondio et al., 2019), several other LOAD-associated loci were found to affect the human lifespan (Tesi et al., 2021). Moreover, several studies reported LOAD risk variants that are associated with both AD and longevity (Bacalini et al., 2022; Dato et al., 2021; Tesi et al., 2021),

emphasizing the importance of studying the pleiotropic effects and epistatic interactions of genetic variants.

Thus, searching for epistatic interactions between variants in genomic regions selected for their association with longevity may help to unravel some of the missing genetic variance of LOAD. To test this hypothesis, we leveraged a large collection of publicly available LOAD GWAS data and conducted gene–gene interaction analysis to find meaningful associations. Genomic regions were prioritized based on previous work by Dato and coworkers (Dato et al., 2018), who analyzed the joint effect on longevity of SNPs belonging to three candidate pathways, the insulin/insulin-like growth factor signaling (IIS), DNA repair, and stress response, respectively. These pathways were chosen as they regulate fundamental biological processes consistently recognized among the most relevant hallmarks of aging from model organisms to humans (Kuningas et al., 2008) and confirmed to have an important role in human longevity in large cohort studies (Deelen et al., 2019).

The analyzed dataset comprised genotypes for a total of 2469 gene variants from 20,766 subjects (11,038 LOAD cases and 9728 controls), belonging to several LOAD cohorts of Northwestern European ancestry. As we stated above growing evidence indicates sex-specific patterns of disease manifestation and sex-dependent effects of *APOE* on LOAD risk. Yet, beyond *APOE*\*4, other genetic risk factors have been found that display sex-specific effects on LOAD, and the interplay between sex and the *APOE* allele has been also explored (Fan et al., 2020). In addition, sex-specific DNA methylation changes in LOAD pathology have been observed (Zhang et al., 2021). On the other hand, also the sex differences in genetic associations with longevity are remarkable (Zeng et al., 2018). Based on this evidence, we reasoned that stratifying genetic association analysis by sex and *APOE* status may facilitate the identification of sex-specific genetic risk loci and ultimately contribute to the understanding of disease heterogeneity between men and women.

## 2 | MATERIALS AND METHODS

### 2.1 | Demographics & study datasets

Fifteen late-Onset Alzheimer's Disease (LOAD) GWAS datasets were obtained from publicly available data repositories (Table 1). Genotyping was performed using various high-density single-nucleotide variant microarrays across cohorts. Participants or their caregivers provided written informed consent in the original studies. The current study protocol was granted an exemption by the Stanford University institutional review board because the analyses were carried out on deidentified, off-the-shelf data.



TABLE 1 Demographic information for individuals in the analysis dataset.

| Cohort      | LOAD   |       | Controls |       | Mean age LOAD (SD) |             | Mean age controls (SD) |             | APOE*4 LOAD |               | APOE*4 controls |             |
|-------------|--------|-------|----------|-------|--------------------|-------------|------------------------|-------------|-------------|---------------|-----------------|-------------|
|             | N      | F     | M        | F     | M                  | F           | M                      | F           | M           | F             | M               |             |
| ACT         | 2,115  | 343   | 190      | 872   | 710                | 81.7 (±6.4) | 80.4 (±6.4)            | 82.5 (±6.1) | 81.7 (±5.9) | 149 (43.4%)   | 91 (47.9%)      | 201 (23.1%) |
| ADCC        | 6,427  | 2,171 | 1,800    | 1,561 | 895                | 74.1 (±8.0) | 72.5 (±7.2)            | 79.5 (±9.0) | 80.1 (±8.6) | 1,411 (65.0%) | 1,201 (66.7%)   | 389 (24.9%) |
| ADDNEUROMED | 239    | 77    | 47       | 64    | 51                 | 73.7 (±7.7) | 74.2 (±6)              | 78.5 (±6.6) | 78.5 (±5.8) | 48 (62.3%)    | 28 (59.6%)      | 17 (26.6%)  |
| ADNI        | 749    | 184   | 247      | 163   | 155                | 74.3 (±6.6) | 75.8 (±6.6)            | 78.7 (±6.4) | 79.6 (±7.4) | 128 (69.6%)   | 168 (68.0%)     | 46 (28.2%)  |
| GenADA      | 1,375  | 400   | 286      | 436   | 253                | 74.0 (±7.3) | 73.9 (±6.2)            | 73.9 (±7.2) | 75.0 (±6.9) | 257 (64.3%)   | 184 (64.3%)     | 100 (22.9%) |
| HBTRC       | 302    | 123   | 100      | 22    | 57                 | 73.9 (±5.5) | 70.3 (±6.1)            | 70.3 (±6.9) | 68.9 (±6.8) | 67 (54.5%)    | 52 (52.0%)      | 5 (22.7%)   |
| NIA-LOAD    | 1,544  | 559   | 311      | 421   | 253                | 72.7 (±6.8) | 71.9 (±6.7)            | 75.3 (±9.4) | 75.8 (±8.6) | 414 (74.1%)   | 236 (75.9%)     | 133 (31.6%) |
| MAYO        | 1,730  | 432   | 292      | 533   | 473                | 73.8 (±5.0) | 73.9 (±5.0)            | 73.7 (±4.5) | 73.4 (±4.3) | 286 (66.2%)   | 192 (65.8%)     | 153 (28.7%) |
| MIRAGE      | 466    | 159   | 97       | 117   | 93                 | 70.6 (±6.4) | 70.8 (±7.0)            | 71.5 (±7.6) | 72.2 (±7.9) | 106 (66.7%)   | 59 (60.8%)      | 42 (35.9%)  |
| OHSU        | 379    | 114   | 64       | 108   | 93                 | 86.9 (±6.3) | 84.6 (±5.1)            | 87.7 (±7.4) | 86.5 (±7.3) | 39 (34.2%)    | 31 (48.4%)      | 23 (21.3%)  |
| ROSMAP      | 1,131  | 468   | 180      | 356   | 127                | 84.3 (±6.6) | 83.8 (±6.5)            | 85.8 (±7.1) | 86.2 (±6.8) | 160 (34.2%)   | 65 (36.1%)      | 74 (20.8%)  |
| TGEN        | 1,012  | 415   | 205      | 188   | 204                | 74.0 (±6.7) | 72.2 (±6.6)            | 82.5 (±8.8) | 79.3 (±8.5) | 277 (66.8%)   | 132 (64.4%)     | 39 (20.7%)  |
| UPIIT       | 1,667  | 627   | 356      | 437   | 247                | 73.2 (±6.8) | 73.0 (±6.5)            | 75.9 (±6.3) | 75.2 (±5.9) | 365 (58.2%)   | 214 (60.1%)     | 84 (19.2%)  |
| UVM         | 1,257  | 354   | 193      | 444   | 266                | 73.6 (±7.7) | 71.5 (±7.3)            | 73.4 (±7.6) | 74.2 (±7.4) | 225 (63.6%)   | 134 (69.4%)     | 111 (25.0%) |
| WASHU       | 373    | 138   | 106      | 86    | 43                 | 76.6 (±6.5) | 75.3 (±8.3)            | 77.6 (±9.9) | 76.5 (±6.6) | 80 (58.0%)    | 55 (51.9%)      | 24 (27.9%)  |
| Total       | 20,766 | 6,564 | 4,474    | 5,808 | 3,920              |             |                        |             |             |               |                 |             |

Abbreviations: F, Females; M, Males.



## 2.2 | Genotyping data: Harmonization & imputation

The entire dataset includes 35,110 participants. Adopted SNP-array Quality Control (QC) procedures were like the ones previously reported (Napolioni et al., 2021). Subjects with autosomal missingness >5% and/or X-chromosome missingness >5% (compared to other subjects in the same dataset), age below 60 years, age information missing, or phenotype inconsistency [missing phenotype, diagnosis of mild cognitive impairment, or a neurodegenerative phenotype other than LOAD] were excluded from the analysis.

Individual ancestry was determined using SNPweights v.2.1 (Chen et al., 2013) by using reference populations from the 1000 Genomes Consortium (1000 Genomes Project Consortium, 2015). By applying an ancestry percentage cut-off  $\geq 80\%$ , the samples were stratified into five super populations, South-Asians (SAS), East-Asians (EAS), Americans (AMR), Africans (AFR), and Europeans (EUR). Since most of the samples belonged to the European population, we also determined their ancestry percentage in the discovery sample according to three genetically distinct European sub-ancestries, Northwestern, Southeastern, and Ashkenazi Jewish, using reference populations available from SNPweights v.2.1. European subjects were stratified into the above-mentioned ancestries when their ancestry percentage was  $\geq 50\%$  for any of the three sub-ancestries. Subjects with genetic ancestry estimates discordant from self-reported ancestry, as well as for subjects showing sex-inconsistency, were excluded from the analyses.

After keeping only the EUR subjects, each GWAS dataset was QCed to remove the SNPs with a call rate  $\leq 95\%$ ; Minor Allele Frequency (MAF)  $\leq 1\%$ ; SNPs with MAF deviating more than 10% from the MAF reported in 1000 Genomes for the EUR population; SNPs with differential missingness between cases and controls ( $p < 0.05$ ); SNPs deviating from Hardy-Weinberg Equilibrium (HWE) in controls ( $p < 5 \times 10^{-5}$ ); tri-allelic SNPs; and SNPs where the alleles are mismatched compared to the 1000 Genomes reference sequence. A/T and C/G SNPs were removed prior to imputation.

All the datasets were phased and imputed using the TopMed Imputation Server (Das et al., 2016). After imputation, variants with a  $r^2$  info score  $\leq 0.75$  were excluded. For the statistical analyses, inter-dataset duplicates (IBD  $> 0.95$ ) were removed from the dataset having the lowest SNP coverage, while, in case of relatedness (IBD  $> 0.0625$ ) the affected or older subjects were kept, independently of SNP coverage.

For association testing analyses, we selected only the Northwestern European subjects since they represented most of the EUR population (approx. 80%) available across the collected GWAS. Analyses were performed using PLINK 2.0 (Chang et al., 2015).

## 2.3 | Selection of candidate genomic regions

Genomic regions harboring the genes selected for longevity in previous work (Dato et al., 2018) were queried. Genetic variants from

the candidate regions were extracted from the full dataset (approx. 12 million variants), considering their hg19 genomic coordinates ( $\pm 10$  kilobases from the gene boundaries), and further filtered by applying a MAF cut-off of 0.05 and genotyping rate of 0.95. The final list of variants was generated by Linkage disequilibrium pruning ( $r^2 > 0.75$ ) to reduce the computational burden of the analysis through the removal of highly correlated variants. Finally, the final dataset comprised a total of 2,469 variants (2,360 SNPs and 109 Ins/dels), as reported in Table S1.

## 2.4 | Statistical analyses

For all the analyses, the whole sample was split based on sex and the presence/absence of APOE\*4, defining four groups: female APOE\*4 carriers, male APOE\*4 carriers, female APOE\*4 non-carriers, and male APOE\*4 non-carriers.

After the QC phase, a logistic regression analysis, with an additive model of association, was performed using PLINK 2.0 on the filtered dataset composed of 20,766 subjects (11,038 LOAD cases and 9,728 controls) and 2,469 variants, to estimate single-marker effects on the predisposition to LOAD. Age, three principal components from the ancestry analysis, APOE\*2 dosage, and study site were used as covariates in the regression models. Results from the univariate analysis of the four study groups were meta-analyzed using GWAMA (Mägi & Morris, 2010). To determine the statistical significance of all the univariate analysis results, a Bonferroni's multiple testing correction was applied [ $(0.05/2469 \text{ variants} \times 4 \text{ study groups})$ ], yielding a  $p$ -value threshold of  $5 \times 10^{-6}$ . A nominal  $p$ -value  $< 0.05$  was used as a filter for the main effect estimation and for selecting the variants to include in the gene-gene interaction analysis carried out using Multifactor dimensionality reduction (MDR) (Ritchie et al., 2001).

$p$ -value distribution enrichment analysis was performed using Pearson's chi-square on two-way contingency tables testing the observed number of variants passing the nominal level of statistical significance ( $p < 0.05$ ) versus the expected one, deeming as statistically significant a Bonferroni's multiple testing correction of  $p < 0.013$  ( $0.05/4 \text{ study groups}$ ) for individual study group or  $p < 0.05$  for the meta-analysis.

To plot single and common variants between groups of samples, Venn diagrams were created with VennDiagram R Package version 1.7.1 (<https://cran.r-project.org/web/packages/VennDiagram/index.html>).

Gene-based association test was performed by Versatile Gene-based Association Study-2 version 2 (VEGAS2, <https://vegas2.qimrb.ergoher.edu.au/>) (Mishra & Macgregor, 2015) particularly useful for analyzing GWAS summary statistics. Based on the association  $p$ -values of the individual variants, VEGAS2 sums the effects of all the variants within a gene and generates a gene-based test statistic by doing simulations of the multivariate normal distribution.

The epistatic interaction of up to four bi-allelic variants was tested using MDR (Ritchie et al., 2001). This methodology estimates high-order interactions among variants, with respect to a given phenotype also when their individual effect is small to moderate,



allowing the discovery of multi-loci genotype combinations associated with high or low disease risk. An entropy-based clustering algorithm sets a contingency table for  $k$  gene variants and calculates case-control ratios for each of the possible multi-loci genotypes; a genotype combination is considered high-level if it is more present in cases compared to controls. For each factor, the MDR interaction model describes percentage of entropy (information gain or IG) and plots a network of two-way interactions, with positive values of entropy indicating synergistic or non-additive interaction while negative entropy values indicate redundancy between the markers or lack of any synergistic interaction between them. In the network, red and orange connections indicate non-linear interactions, green and brown connections indicate independence or additivity, and blue connections indicate redundancy. For all 2-order, 3-order, or 4-order combinations, the best model is considered the one found more consistent in different replicates (expressed as CV, consistency values and accuracy, i.e., training balanced accuracy level). To calculate significance, permutation testing was applied, dividing the data set into 10 portions, and using nine portions as a training data set, and the remaining as a testing data set. Ten thousand permutations were performed, to determine a cutoff threshold for an  $\alpha=0.05$  significance level. For each order of interaction tested, an odds ratio (OR) is outputted, referring to the best combination of variants (best model), while determining the multi-locus high-risk combinations.

Multifactor dimensionality reduction analyses were implemented in the open-source MDR software package version 3.0.2 (<https://sourceforge.net/projects/mdr/>).

## 2.5 | Functional annotation

Functional annotation of risk variants was performed by using multiple bioinformatic tools and databases, including the HaploReg database (<https://pubs.broadinstitute.org/mammals/haploreg/haploreg.php>), the GTEX portal (<https://gtexportal.org/home/>), RegulomeDB database (<https://beta.regulomedb.org/regulome-search/>) version 2.1, SNP Nexus (<https://www.snp-nexus.org/v4/>), and MetaBrain (<https://www.metabrain.nl/cis-eqtl.html>). LDlink's LDproxy tool (<https://analysistools.nci.nih.gov/LDlink/>) (Machiela & Chanock, 2015) and European population data was used for SNP LD analysis.

## 3 | RESULTS

### 3.1 | Single-variant and gene-based analysis

The flowchart in Figure 1 details the study design. After quality control and filtering, we performed logistic regression analysis on the sample divided in four sub-groups according to sex- and APOE\*4

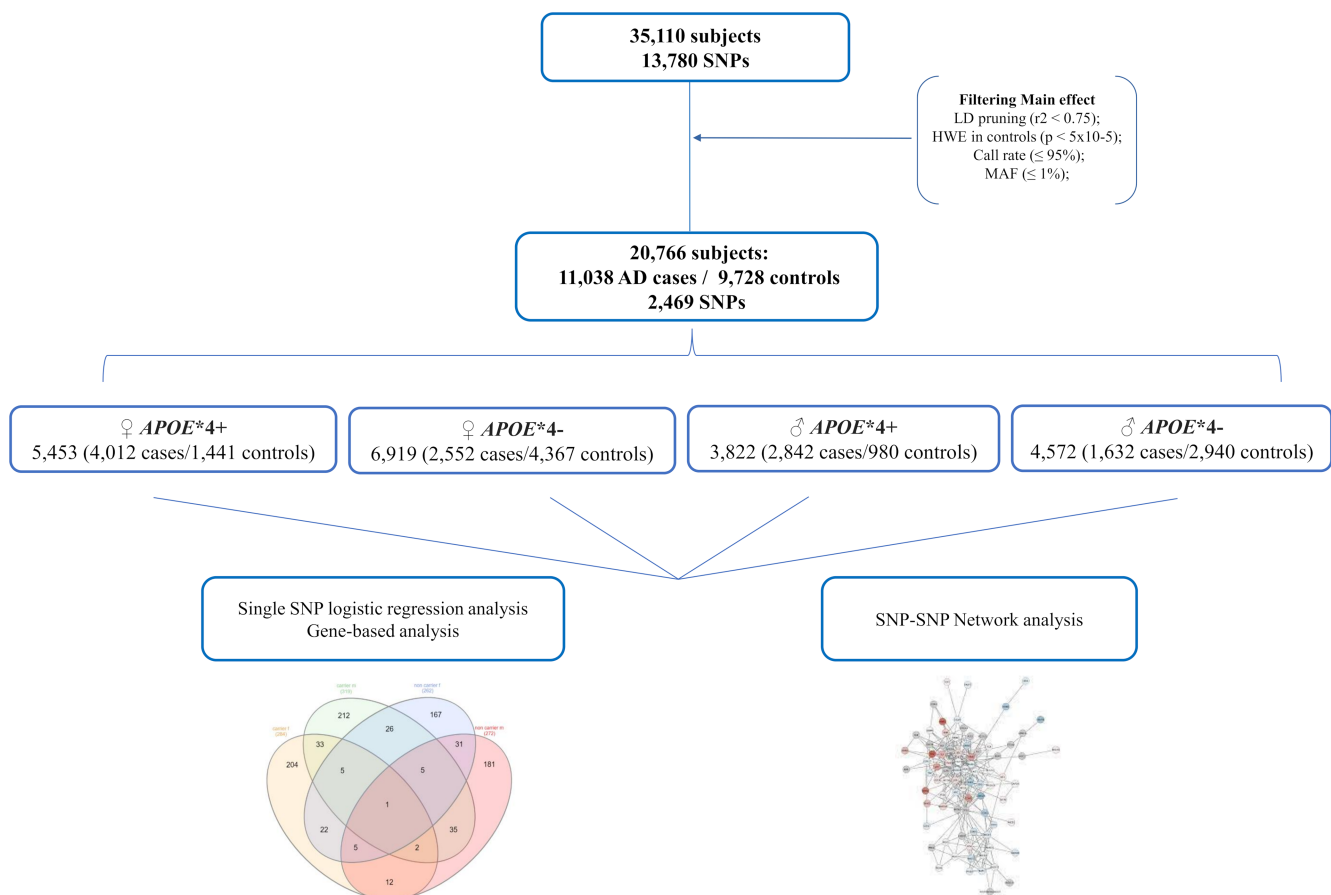


FIGURE 1 Flowchart describing the steps of the analysis after quality control and filtering.



status, and meta-analyzing them thereafter. In Table S2 we reported the variants associated with the disease risk at a nominal  $p$ -value, along with their chromosomal location, the assigned gene and the main functional pathway associated with each coded protein. A graphical representation of all the obtained  $p$ -values is presented as a Manhattan plot (Figure S1). These associations, however, did not stand upon correction for multiple comparisons ( $p < 5 \times 10^{-6}$ ) either when considering the single study group or when meta-analyzed across the four study groups. Nonetheless, we observed a statistically significant 45% enrichment ( $p = 0.002$ ) in the distribution of nominally significant variants ( $p < 0.05$ ) when the four study groups were meta-analyzed (Table 2), even though no statistically significant enrichment was found when analyzing individually the four study groups. Interestingly, we also detected a statistically significant enrichment from the meta-analysis Cochran's heterogeneity statistic's  $p$ -values ( $p = 0.020$ , Table 2), supporting the existence of  $APOE^*4$  and sex-specific effects.

Within the four study groups, the nominally associated variants belong to 126 different genes, of which 20 are in the IIS, 31 in DNA repair, and 23 in stress response pathways, whereas the remaining

46 are related to other pathways, such as immunity and membrane trafficking (see Table S2). These last genes emerged probably because of a high gene density and/or overlapping genes in some of the genomic regions considered, which extend 10kb upstream and downstream of the candidate gene boundaries.

More specifically, the variants significantly associated in the sub-groups were: 148 in  $APOE^*4^+$  females, 157 in  $APOE^*4^+$  males, 115 in  $APOE^*4^-$  females, and 136 in  $APOE^*4^-$  males. The top-variants ( $p < 0.001$ ) were: rs17810889-*C8orf49* and rs5742665-*IGF1* in  $APOE^*4^+$  females, rs56190996-*IGF1R* and rs8113762-*IRGQ* in  $APOE^*4^+$  males, rs28362737-*AQP1* and rs35519594-*XDH* in  $APOE^*4^-$  females, rs3729587-*XPC* and rs142270994-*CTD-3094K11.1* in  $APOE^*4^-$  males. The Venn diagram for the gene variants listed in Table S2 shows the number of variants in each sub-group and those shared (Figure 2). As it is shown in Table 3, 12 variants were associated with LOAD risk in females, independently from  $APOE^*4$  status, five of which showed an opposite direction of effect in the two sub-groups (Table 3a). In males, eight variants were associated with LOAD independently from  $APOE^*4$  status, five of them showing a divergent effect in the two sub-groups (Table 3b). On the other

| Group  | N of variants with $p < 0.05$ | OR    | Enrichment $p$ |
|--|-------------------------------|-------|----------------|
| $APOE^*4^+$ females                            | 148 (6.0%)                    | 1.216 | 0.118          |
| $APOE^*4^+$ males                              | 157 (6.4%)                    | 1.295 | 0.036          |
| $APOE^*4^-$ females                            | 115 (4.7%)                    | 0.932 | 0.597          |
| $APOE^*4^-$ males                              | 136 (5.5%)                    | 1.112 | 0.406          |
| Meta-analysis                                  |                               |       |                |
| Meta-analysis $p$ -value                       | 174 (7.1%)                    | 1.446 | <b>0.002</b>   |
| Cochran's heterogeneity statistic's $p$ -value | 161 (6.5%)                    | 1.331 | <b>0.020</b>   |

TABLE 2  $p$ -value distribution enrichment analysis performed across the four study groups and the meta-analysis results.

Note: We deemed as statistically significant a Bonferroni's multiple testing correction of  $p < 0.013$  ( $0.05/4$  study groups) for individual study group or  $p < 0.05$  for the meta-analysis.  $p$ -values reported in bold are statistically significant.

Abbreviations: OR, odds ratio;  $p$ ,  $p$ -value.

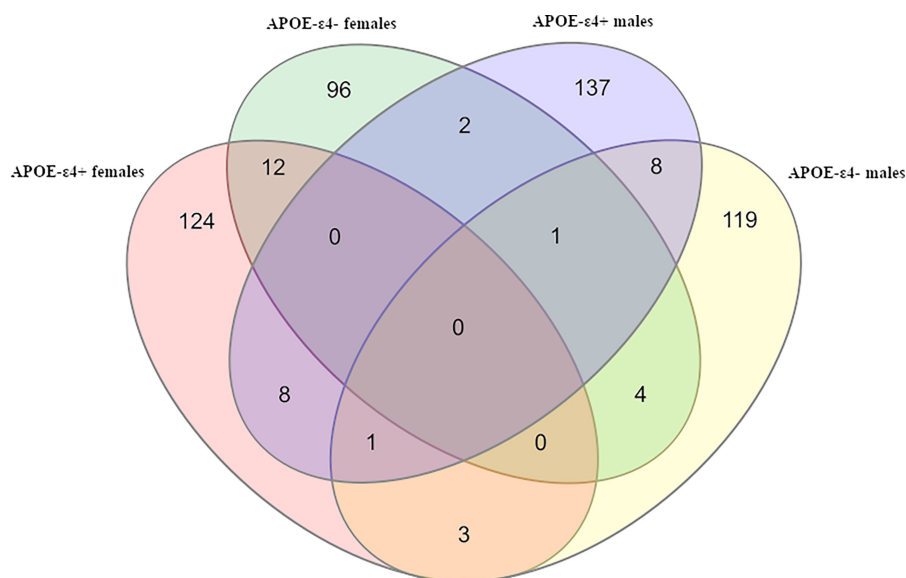


FIGURE 2 VENN diagram built on Table S1 data, showing the number of variants associated with LOAD in each sub-group of samples and in common between different groups.



**TABLE 3** Gene variants nominally associated with LOAD, shared between: (A) *APOE*\*4<sup>+</sup> females and *APOE*\*4<sup>-</sup> females; (B) *APOE*\*4<sup>+</sup> males and *APOE*\*4<sup>-</sup> males; (C) *APOE*\*4<sup>+</sup> females and *APOE*\*4<sup>+</sup> males; (D) *APOE*\*4<sup>-</sup> females and *APOE*\*4<sup>-</sup> males.

| Variant     | Chr. | Position    | Gene SYMBOL         | EA | OR                                | <i>p</i> | OR                                | <i>p</i> |
|-------------|------|-------------|---------------------|----|-----------------------------------|----------|-----------------------------------|----------|
|             |      |             |                     |    | <b>APOE*4<sup>+</sup> females</b> |          | <b>APOE*4<sup>-</sup> females</b> |          |
| <b>A</b>    |      |             |                     |    |                                   |          |                                   |          |
| rs13183641  | 5    | 95,147,287  | <i>RHOBTB3</i>      | T  | 0.873                             | 0.003    | 0.909                             | 0.010    |
| rs4561      | 5    | 95,152,313  | <i>RHOBTB3</i>      | G  | 0.886                             | 0.008    | 0.910                             | 0.011    |
| rs2348974   | 5    | 95,143,394  | <i>RHOBTB3</i>      | C  | 1.119                             | 0.015    | 1.093                             | 0.014    |
| rs6556881   | 5    | 95,134,419  | <i>RHOBTB3</i>      | G  | 0.908                             | 0.038    | 0.925                             | 0.034    |
| rs34886287  | 5    | 80,077,309  | <i>MSH3</i>         | C  | 1.110                             | 0.029    | 1.105                             | 0.007    |
| rs2645429   | 8    | 11,660,051  | <i>FDFT1</i>        | A  | 1.111                             | 0.048    | 0.902                             | 0.016    |
| rs2645433   | 8    | 11,657,921  | <i>RP11-297N6.4</i> | C  | 0.902                             | 0.027    | 1.081                             | 0.035    |
| rs112267867 | 9    | 118,905,353 | <i>PAPPA</i>        | A  | 1.260                             | 0.037    | 1.179                             | 0.044    |
| rs6583817   | 10   | 94,247,247  | <i>IDE</i>          | T  | 0.836                             | 0.006    | 0.859                             | 0.005    |
| rs4752254   | 10   | 120,910,136 | <i>SFXN4</i>        | C  | 0.895                             | 0.042    | 1.094                             | 0.036    |
| rs2860173   | 19   | 7,129,086   | <i>INSR</i>         | A  | 1.230                             | 0.016    | 0.870                             | 0.039    |
| rs12979722  | 19   | 7,118,878   | <i>INSR</i>         | C  | 1.169                             | 0.042    | 0.846                             | 0.006    |
|             |      |             |                     |    | <b>APOE*4<sup>+</sup> males</b>   |          | <b>APOE*4<sup>-</sup> males</b>   |          |
| <b>B</b>    |      |             |                     |    |                                   |          |                                   |          |
| rs78686161  | 1    | 242,065,356 | <i>EXO1</i>         | A  | 1.450                             | 0.005    | 1.303                             | 0.006    |
| rs670548    | 6    | 53,366,989  | <i>GCLC</i>         | C  | 0.859                             | 0.009    | 1.123                             | 0.015    |
| rs7740677   | 6    | 46,649,231  | <i>SLC25A27</i>     | C  | 1.167                             | 0.030    | 1.154                             | 0.013    |
| rs17069665  | 6    | 108,941,468 | <i>FOXO3</i>        | G  | 0.832                             | 0.033    | 1.169                             | 0.031    |
| rs2684794   | 15   | 99,484,953  | <i>IGF1R</i>        | C  | 0.848                             | 0.038    | 1.135                             | 0.049    |
| rs7245548   | 19   | 45,981,840  | <i>ERCC1</i>        | T  | 1.126                             | 0.036    | 0.912                             | 0.049    |
| rs4803825   | 19   | 45,986,483  | <i>RTN2</i>         | G  | 0.889                             | 0.042    | 1.128                             | 0.012    |
| rs4328554   | 19   | 7,249,830   | <i>INSR</i>         | T  | 1.129                             | 0.046    | 1.130                             | 0.014    |
|             |      |             |                     |    | <b>APOE*4<sup>+</sup> females</b> |          | <b>APOE*4<sup>+</sup> males</b>   |          |
| <b>C</b>    |      |             |                     |    |                                   |          |                                   |          |
| rs17882672  | 6    | 53,408,883  | <i>GCLC</i>         | T  | 0.858                             | 0.018    | 1.236                             | 0.018    |
| rs7092649   | 10   | 60,005,202  | <i>IPMK</i>         | A  | 0.878                             | 0.017    | 0.866                             | 0.037    |
| rs17636964  | 10   | 59,953,046  | <i>IPMK</i>         | C  | 1.139                             | 0.025    | 1.167                             | 0.029    |
| rs1625716   | 10   | 59,960,083  | <i>IPMK</i>         | G  | 0.826                             | 0.038    | 0.784                             | 0.033    |
| rs7138318   | 12   | 104,736,394 | <i>TXNRD1</i>       | C  | 0.861                             | 0.002    | 1.146                             | 0.024    |
| rs7979495   | 12   | 104,625,779 | <i>TXNRD1</i>       | G  | 0.810                             | 0.018    | 1.247                             | 0.047    |
| rs141516621 | 19   | 7,280,152   | <i>INSR</i>         | A  | 1.232                             | 0.003    | 0.844                             | 0.043    |
| rs7258382   | 19   | 7,262,569   | <i>INSR</i>         | C  | 1.141                             | 0.048    | 0.841                             | 0.027    |
|             |      |             |                     |    | <b>APOE*4<sup>-</sup> females</b> |          | <b>APOE*4<sup>-</sup> males</b>   |          |
| <b>D</b>    |      |             |                     |    |                                   |          |                                   |          |
| rs2010704   | 2    | 31,622,465  | <i>XDH</i>          | A  | 1.098                             | 0.011    | 1.106                             | 0.030    |
| rs147249797 | 2    | 31,601,541  | <i>XDH</i>          | T  | 1.092                             | 0.034    | 1.123                             | 0.029    |
| s10759223   | 9    | 110,065,158 | <i>RAD23B</i>       | C  | 1.078                             | 0.038    | 0.909                             | 0.041    |
| rs2494741   | 14   | 105,249,322 | <i>AKT1</i>         | T  | 1.157                             | 0.032    | 0.754                             | 0.002    |

Abbreviations: EA, effect allele; OR, Odds Ratio; *p*, *p*-value.

hand, *APOE*\*4 carriers, independent of sex, share eight markers, five of which show an opposite effect in the two sexes (Table 3c), while *APOE*\*4<sup>-</sup> share four markers, two of which show an opposite effect in the two sexes (Table 3d).

For testing the enrichment of associated variants in the same gene, we then performed a gene-based analysis using VEGAS2. Table S3 reports the top-genes (*p* < 0.01) and the top-variant associated with the disease risk in the four sub-groups of samples. The schematic representation of Table S3 data is reported in Figure 3. The *INSR*

gene is the only one common to all the sub-groups, although through different variants. *FDFT1* and *MSH3* were the top-genes in females, while *IGF1R*, *IGF2R*, *PAPPA*, *GCLC*, and *XPC* genes were the top-genes in males, independent of *APOE*\*4 status. These genes, thus, appear to be associated with LOAD in a sex-specific way. Conversely, *APOE*\*4<sup>+</sup> subjects, independent of by sex, share markers in *IGF1R*, *GCLC*, and *IPMK* genes; *APOE*\*4<sup>-</sup> subjects, by contrast show an enrichment of significant markers in *IGF2R*, *AKT1*, *GSR*, *MSH3*, and *XDH* genes, suggesting them as influenced by *APOE* status in LOAD susceptibility.

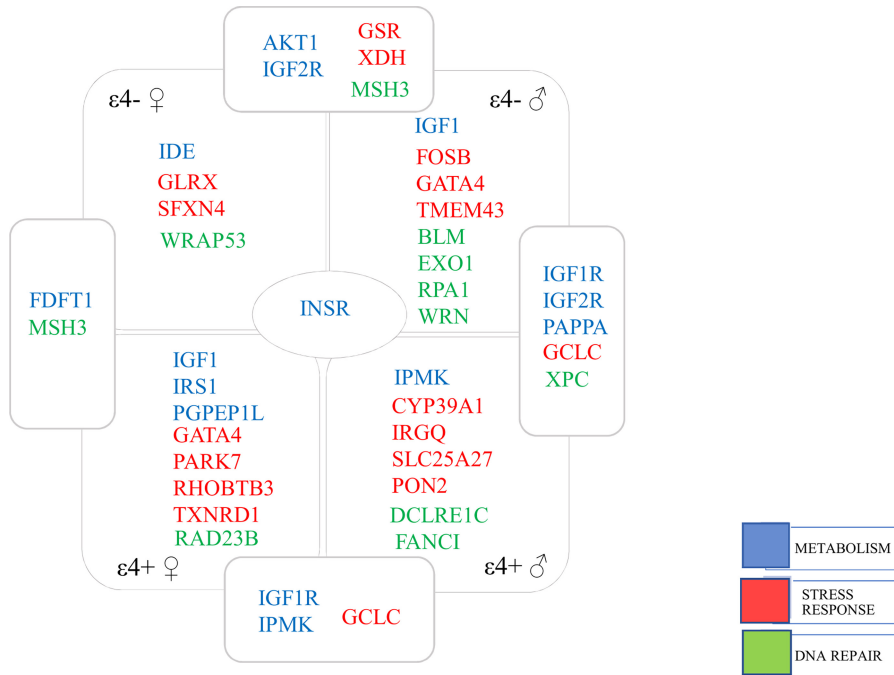


**FIGURE 3** Schematic representation of gene-based analysis, reporting the top-genes ( $p < 0.01$ ) associated with the disease in each different sub-group and those shared. Colors represent the three analyzed pathways.

### 3.2 | Analysis of epistatic interactions

With the aim of finding gene–gene epistatic interactions between 2- or among 3- and 4-markers associated with the disease risk, we used the MDR approach. Table 4 shows the gene–gene interactions for LOAD resulting from the analysis, while Figure 4 depicts the interaction networks between variants in each sub-group.

In  $APOE^*4^+$  females, two 2-order epistatic interactions (Figure 4a) were found significantly associated with LOAD, namely the combinations rs3757949-GATA4/rs7092522-IDE and rs62491484-NEIL2/rs35435718-PGPEP1L. These four variants were among the most significant associated with LOAD ( $p < 0.01$ ) in this sub-group for the single-variant analysis. Both epistatic interactions were inter-pathway, combining markers of genes belonging, respectively, to stress response (GATA4) and metabolism (IDE), and to DNA repair (NEIL2) and stress response (PGPEP1L). The same pathways also emerged from the 3- and 4-order loci interactions (Table 4a), where two markers of the gene TXNRD1 (rs28672744 in the 3-order and rs35511346 in the 4-order interactions) and one of FDFT1 (rs26861869) are included. As indicated by the interaction graph in Figure 4a, several variants show a redundant effect (blue lines) in the network. Among them, the rs5742665-IGF1 is the top-variant from the gene-based analysis in this sub-group ( $p < 0.001$ ; Table S2) and seems to be a LOAD specific marker of  $APOE^*4^+$  females, not being associated with disease in the other sub-groups.

No significant epistatic interactions were observed in the group of  $APOE^*4^-$  females (Figure 4b). The variant rs28362737-AQP1 present in the network is the most associated with LOAD in this group, but it seems to have a univariate effect.

In  $APOE^*4^+$  males (Figure 4c), the most important gene–gene interactions (red lines) were: rs4674302-AOX1/rs718630-PTPN1 and rs56190996-IGF1R/rs4325676-INSR. These interactions are driven

by rs718630-PTPN1 and rs56190996-IGF1R variants, which are the most significantly associated with LOAD ( $p < 0.01$ ) in the single-marker analysis, with the last representing the top-variant in IGF1R associated with LOAD in the subgroup. Both interactions are intra-pathway epistasis between genes involved in metabolism. The 3-order interaction is again an intra-pathway epistasis, involving AOX1, GCLC, and KCL3 genes whose products act in metabolism.

In  $APOE^*4^-$  males (Figure 4d), two gene–gene interactions resulted from MDR analysis namely rs11573680-RAD32B/rs4983559-ZBTB42, relative to the DNA-repair pathway, and rs6214-IGF1/rs1879612-IGF1R to metabolism. 3-order and 4-order interactions resume the collaboration of DNA repair and metabolism, in addition to stress response pathway, in the susceptibility to LOAD in this sub-group.

To determine whether the gene–gene interactions found were exclusive between the four sub-groups, we ran MDR using those selected interactions across all the groups. Notably, we observed that the rs62491484-NEIL2/rs35435718-PGPEP1L epistatic interaction found in  $APOE^*4^+$  females occurred also in  $APOE^*4^-$  males ( $p = 0.028$ ) (Table 4). However, the high-risk genotypic combinations were not comparable (Figure S2). Similarly, the rs11573680-RAD32B/rs4983559-ZBTB42 interaction found in  $APOE^*4^-$  males occurred also in the  $APOE^*4^+$  males ( $p = 0.038$ ) (Table 4), although with a different pattern of high-risk genotypic combinations (Figure S2).

### 3.3 | Functional annotation analysis

Next, we performed functional annotation to ascertain biological significance of the variants identified in the single variant and interaction analyses. To this end, several databases and tools

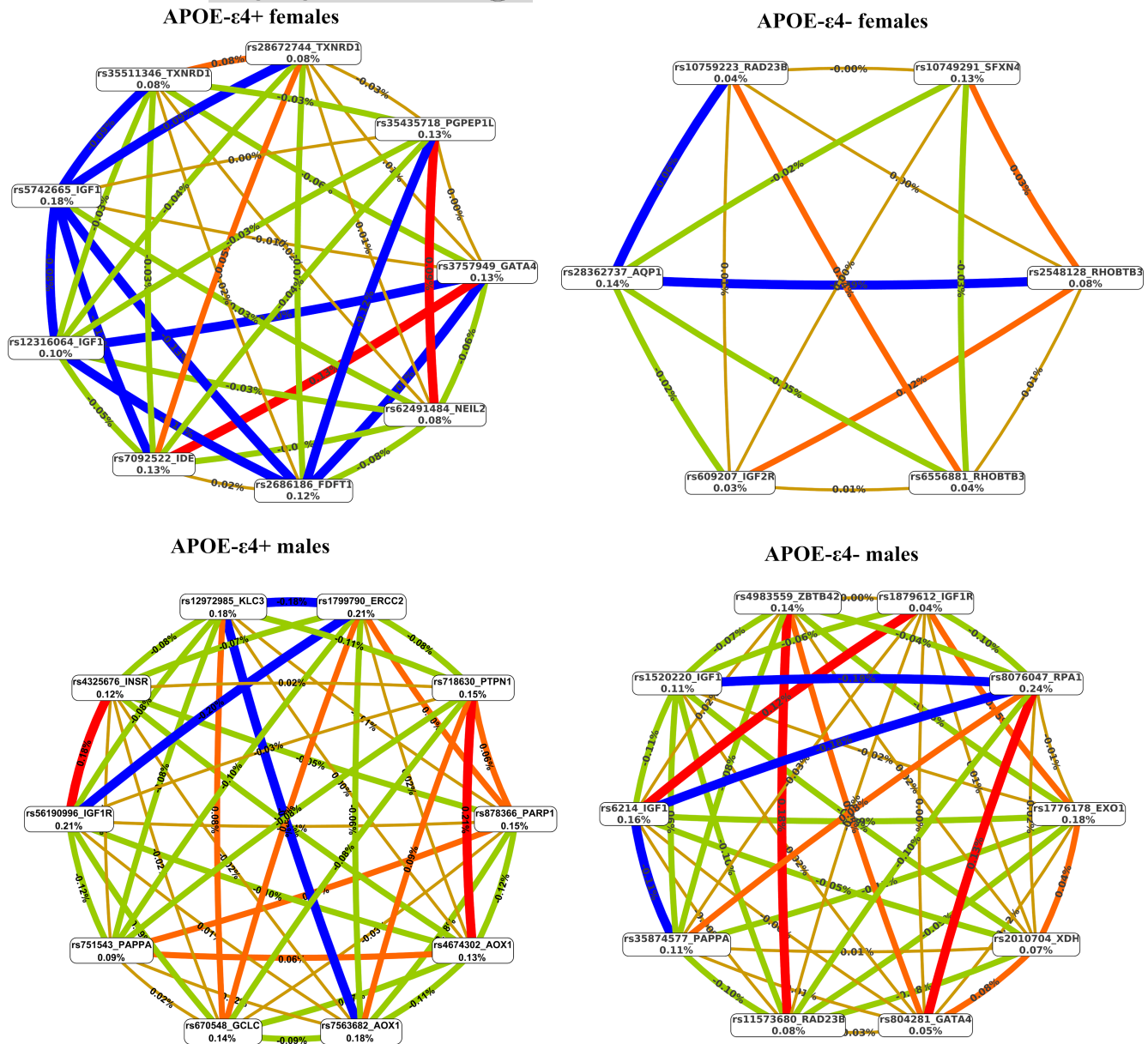




TABLE 4 Significant results of gene-gene interaction associations, resulting from the MDR analysis.

|                                      | Gene-gene combination                             | Genes included in the combination | Pathways involved                            | OR(95% CI.)       | p-value (10,000 permutations) |                           |                             |                           |
|--------------------------------------|---|-----------------------------------|--|-------------------|-------------------------------|---------------------------|-----------------------------|---------------------------|
|                                      |   |                                   |  |                   | APOE*4 <sup>+</sup> females   | APOE*4 <sup>+</sup> males | APOE*4 <sup>-</sup> females | APOE*4 <sup>-</sup> males |
| <b>A: APOE*4<sup>+</sup> females</b> |   |                                   |  |                   |                               |                           |                             |                           |
| 2-order interactions                 | rs3757949/rs7092522                               | GATA4/IDE                         | Stress response/<br>Metabolism               | 1.42 (1.25, 1.62) | 0.0001                        | 0.1945                    | 0.7051                      | 0.6106                    |
|                                      | rs62491484/rs35435718                             | NEIL2/PGPEP1L                     | DNA repair/Stress<br>response                | 1.36 (1.19, 1.54) | 0.0002                        | 0.6143                    | 0.8744                      | 0.0294                    |
| 3- and 4-order interactions          | rs62491484/rs28672744/<br>rs35435718              | NEIL2/TXNRD1/PGPEP1L              | DNA repair/Stress<br>response                | 1.56 (1.38, 1.76) | 0.0001                        | 0.8034                    | 0.9658                      | 0.4729                    |
|                                      | rs2686186/rs7092522/<br>rs12316064/<br>rs35511346 | FDF1/IDE/IGF1/TXNRD1              | Stress response/<br>Metabolism               | 1.96 (1.72, 2.22) | 0.0001                        | 0.9389                    | 0.6944                      | 0.8240                    |
| <b>B: APOE*4<sup>+</sup> males</b>   |   |                                   |  |                   |                               |                           |                             |                           |
| 2-order interactions                 | rs4674302/rs718630                                | AOX1/PTPN1                        | Stress response/<br>Metabolism               | 1.46 (1.27, 1.69) | 0.8127                        | 0.0001                    | 0.9709                      | 0.9489                    |
|                                      | rs56190996/rs4325676                              | IGF1R/INSR                        | Metabolism                                   | 1.49 (1.28, 1.73) | 0.5017                        | 0.0002                    | 0.2057                      | 0.2499                    |
| 3- order interaction                 | rs7563682/rs670548/<br>rs12972985                 | AOX1/GCLC/KLC3                    | Stress response/<br>Metabolism               | 1.69 (1.46, 1.96) | 0.9976                        | 0.0001                    | 0.9992                      | 0.2060                    |
| <b>C: APOE*4<sup>-</sup> males</b>   |   |                                   |  |                   |                               |                           |                             |                           |
| 2-order interactions                 | rs11573680/rs4983559                              | RAD23B/ZBTB42                     | DNA repair                                   | 1.43 (1.24, 1.64) | 0.7629                        | 0.0318                    | 0.7856                      | 0.0004                    |
|                                      | rs6214/rs1879612                                  | IGF1/IGF1R                        | Metabolism                                   | 1.33 (1.18, 1.50) | 0.6723                        | 0.8911                    | 0.5558                      | 0.0004                    |
| 3- and 4-order interactions          | rs11573680/rs1520220/<br>rs4983559                | RAD23B/IGF1/ZBTB42                | DNA repair/<br>Metabolism                    | 1.55 (1.37, 1.76) | 0.2953                        | 0.8032                    | 0.9899                      | 0.0001                    |
|                                      | rs1776178/rs2010704/<br>rs804281/rs1879612        | EXO1/XDH/GATA4/IGF1R              | DNA repair/Stress<br>response/<br>Metabolism | 1.16 (1.09, 1.40) | 0.5058                        | 0.9903                    | 0.9301                      | 0.0003                    |

Note: 2- 3- and 4-loci interactions are shown, with respective pathways, selected for CV (10/10 replicates) and training balanced accuracy (>0.5). The OR value of the best combination of variants (best model) is reported. p-values reported in bold are considered statistically significant.



**FIGURE 4** Interaction graphs, reporting the significant markers from MDR analysis, in the group of  $APOE^*4^+$  females (a), in  $APOE^*4^-$  females, in  $APOE^*4^+$  males, and in  $APOE^*4^-$  males (d). For each variant we reported the value of information gain (IG) in per cent, while numbers in the connections indicate the entropy-based IG for the variant pairs. Red bar and orange bar indicate the high-level synergies on the phenotype, while the brown indicate a medium-level interaction, green and blue connections with negative IG values indicate redundancy or lack of synergistic interactions between the markers.

were considered, as reported in the Materials & Methods section. [Table S4](#) reports the most relevant results of eQTL analysis of the associated variants and their proxies in high LD ( $r^2 \geq 0.8$ ). According to this analysis some of the risk variants act as cis-eQTL regulatory elements which modulate the expression of the corresponding gene or of nearby genes in specific brain regions. Moreover, evidence of a regulatory role (1f or 1b score in RegulomeDb and association with regulatory elements in SNPnexus) was found for other variants associated with the disease phenotype.

Some variants reported a relevant number of proxies in LD ( $r^2 \geq 0.8$ ), although none showed evidence of stronger regulatory potential than the lead variant. As reported in [Table S4](#), the significant variants we

identified were not previously implicated in LOAD, yet some of them have been reported to affect some age-related disorders.

## 4 | DISCUSSION

The genetic architecture of LOAD has been widely studied in recent years, and so far, 100 of risk genes and related rare and common genetic variants have been identified, but many remain to be uncovered (Andrews et al., 2023). As advanced age is the greatest risk factor for LOAD, shared genetic pathways between LOAD and longevity are expected, although their connections are still not fully



understood (Tesi et al., 2021). Phenotypic heterogeneity (i.e., distinct groups of subjects present with different clinical syndromes) and/or temporal heterogeneity (i.e., substantial inter-subject variance in age-at-onset and rate of decline) (Young et al., 2018) are common in LOAD. Another challenge is the small contribution of individual genetic variants in complex phenotypes. Moreover, several studies have emphasized that genetic interactions may be more important than single markers in neurodegenerative diseases and longevity (Gilbert-Diamond & Moore, 2011), suggesting the existence of non-additive heritability to these traits.

In this study, we applied a gene–gene interaction approach to a set of genetic variants selected for being on or near genes involved in the IIS, the DNA repair, and the oxidative stress response pathways, previously linked to human longevity (Dato et al., 2018). To identify gene signatures for LOAD related to sex and/or to APOE genotype, we performed analyses stratified by APOE\*4 status and sex. The validity of the choice of such study design was underscored by additional cross-validation analyses, which confirmed the presence of heterogeneity across the different sub-groups.

Overall, this study highlights two aspects of the genetic complexity in LOAD. First, it supports the claim of shared genetic pathways between longevity and LOAD. Second, it suggests that sex and APOE genotype can drive different genetic risk factors. This evidence appeared clear in single variant analyses. In APOE\*4<sup>+</sup> females, the two top variants were rs17810889 upstream of *C8orf49*, and rs5742665 in an intron of *IGF1* gene, one of the master genes in IIS metabolic pathway. In APOE\*4<sup>-</sup> females, the top-variant was rs28362737, an intronic variant of *AQP1*, the gene encoding Aquaporin 1, a protein associated with amyloid-beta deposition in AD brains (Misawa et al., 2008). In APOE\*4<sup>+</sup> males, the top-variants were rs56190996, in an intron of *IGF1R* (insulin-like growth factor receptor), and rs8113762 located at the 3'-UTR of *IRGQ* (immunity-related GTPase Q), while in APOE\*4<sup>-</sup> subjects, the most significant variant was rs3729587 in the DNA repair gene *XPC* (Xeroderma pigmentosum, complementation group C). Many of these markers appear to be functionally relevant, being cis-eQTL or trans-eQTL, and specifically in brain regions, as reported in Table S4. However, we cannot exclude that one of their proxies in LD ( $r^2 \geq 0.8$ ) could be the actual causal variant, although none showed a potential regulatory effect higher than the associated variants.

It is also worth noting that some of the associated variants showed an opposite effect in the two sexes. This is line with several studies demonstrating that some variants, the so-called “sexually antagonistic variants”, have a beneficial effect in one sex but deleterious (or null) effects in the other, thus having a role in shaping differences between males and females in age-related disease outcomes as well as in survival (Iannuzzi et al., 2023; Lagou et al., 2021).

Results from gene-based analysis further highlighted genes associated with LOAD in a sex- and APOE-specific manner. *INSR*, is the only one gene shared among the four sub-groups of patients, which encodes the insulin receptor, an important component of the insulin pathway. Through its binding with insulin, *INSR* controls the glucose metabolism in the brain helping to maintain neuronal functioning

(de la Monte & Wands, 2005). Decline in glucose metabolism is indeed one of the earliest and most common anomalies observed in patients with LOAD (Akhtar & Sah, 2020). A recent study by Leclerc et al. (2023) reported that, in association with  $\beta$ -amyloid pathology, defects in the activation of *INSR* at the blood–brain barrier strongly contribute to brain insulin resistance in LOAD. Genetic variants of this gene were found enriched in centenarians, thus indicating *INSR* a key mediator of human longevity (Barbieri et al., 2003).

The evaluation of the joint effect of different markers through gene–gene interactions further added insights into the genetic architecture of LOAD. Among the significantly interacting genes, *PTPN1* (protein tyrosine phosphatase non-receptor type 1, IIS pathway), *TXNRD1* (thioredoxin reductase 1; stress response), and *IGF1R* (insulin-like growth factor 1 receptor; IIS) were already found in combinations affecting survival to old age (Dato et al., 2018; Ukraintseva et al., 2021). *PTPN1* and *TXNRD1* were engaged in best risk combinations for longevity, respectively, with *IGF1R* and *TP53* (DNA repair), while *IGF1R*, interacted with *TP53* and *TGFBR2* (cell proliferation). In LOAD *PTPN1* interacts with a partner from the stress response pathway, like *AOX1*. Notably, *TXNRD1* is engaged in 4-order risk combination for LOAD with genes from the IIS pathway, like *IGF1*, *FDFT1* (farnesyl-diphosphate farnesyltransferase 1), and *IDE* (insulin degrading enzyme). Similarly, *IGF1R* is associated with the disease in a 4-order synergic combination with *EXO1* (DNA repair), *XDH* (stress response), and *GATA4* (IIS), behind its ligand *IGF1*. Overall, these findings suggest that in LOAD as in longevity *TXNRD1* and even more *IGF1R*, may represent hubs interconnecting multiple signaling pathways. The different sub-processes may instead explain the sex- and APOE-specific associations we found.

Taken together, these results suggest that longevity loci may also drive LOAD neuropathology through APOE- and sex-related specific gene–gene interactions. The complex interplay among sex, APOE, and age may influence the severity and the temporal trajectory of LOAD progression, creating a risk profile for LOAD that could serve to identify high-risk individuals (Riedel et al., 2016). Mechanisms underlying the sex differences are unknown; the literature largely supports the claim that it may be due to the known differences in longevity between men and women (Hossin, 2021), while some propose that sex dimorphisms in stress responses can contribute to the increased prevalence of LOAD in women (Yan et al., 2018). Sex divergence in biochemical responses to stress were reported along the hypothalamic–pituitary–adrenal axis and in the activation of the cortical corticotrophin-releasing factor receptor 1 signaling pathway, leading to distinct female-biased increases in molecules associated with LOAD pathogenesis (Yan et al., 2018). In our analysis, effectors of stress response, such as *TXNRD1* and *GATA4*, have been found in all the sub-groups of patients, suggesting that an impaired ability to induce a stress response represents an underlying risk factor for LOAD. Interestingly, in APOE\*4<sup>+</sup> females, potentially experiencing higher levels of hydroxyl radicals and reduced levels of mitochondrial antioxidants compared to non-APOE\*4 carriers (Ihara et al., 2000), all significant epistatic interactions were among genes involved in oxidative stress and those belonging to the other pathways.



## 5 | CONCLUSIONS

Collectively, the present results indicate that several loci repeatedly implicated in aging and longevity also contribute to late-onset Alzheimer's disease (LOAD) risk. Most of the top genes associated are assigned to pathways related to metabolism, highlighting their relevance both in the aging process and the pathological events leading to LOAD. Interestingly, this study bolsters the evidence of specific interactions among established risk factors for LOAD, that is APOE genotype and sex, and these genes. This suggests that different trajectories of cognitive aging may be the result of specific epistatic effects between genetic and non-genetic risk factors. Although our conclusions are based on the evidence of "statistical epistasis", which magnitude and contribution to the variance of complex traits is a highly debated topic (Hivert et al., 2021), in accordance with other authors (Singhal et al., 2023) we think that the potential for "functional epistasis" to drive expressivity and explain clinical heterogeneity in complex diseases is mounting. In the complex scenario of LOAD, understanding the functional changes associated with different combinations of interacting entities (SNPs, genes, pathways, etc.) may help to disentangle the genetic architecture underlying disease development, and interindividual differences that underpin disease, finally leading to precision medicine approaches for early detection of individuals at higher risk for cognitive decline or dementia.

### AUTHOR CONTRIBUTIONS

Idea/concept: SD, FDR, GR, VN; Data curation/processing: VN, SP, MEB, YLG; Data analysis: SD, FDR, PC, GR, VN; Writing: SD, FDR, PC, GR, VN; Advice: MEB, YLG, MDG, GP.

### ACKNOWLEDGMENTS

This research was supported by "S.I.F.I.PA.CRO.DE.-Sviluppo e industrializzazione farmaci innovativi per terapia molecolare personalizzata PA.CRO.DE." PON ARS01\_00568 granted by MIUR (Ministry of Education, University and Research) Italy to G.P. and by grants from NIH K99AG075238 (MEB), P30AG066515 Development project (MEB), and the Alzheimer's Association (AARF-20-683984, MEB). The work has been made possible by the collaboration with Gruppo Baffa (Sadel Spa, Sadel San Teodoro srl, Sadel CS srl, Casa di Cura Madonna dello Scoglio, AGI srl, Casa di Cura Villa del Rosario srl, Savelli Hospital srl, Casa di Cura Villa Ermelinda). Biological samples used in this study were stored at principal investigators' institutions and at the National Cell Repository for Alzheimer's Disease (NCRAD) at Indiana University, which receives government support under a cooperative agreement grant (U24 AG21886) awarded by the National Institute on Aging (NIA). We thank contributors who collected samples used in this study, as well as patients and their families, whose help and participation made this work possible. Phenotypic data were provided by principal investigators, the NIA funded Alzheimer's Disease Centers (ADCs), and the National Alzheimer's Coordinating Center (NACC). Genetic data were contributed by principal investigators on projects that were individually

funded by NIA, other NIH institutes, private U.S. organizations, or foreign governmental or nongovernmental organizations. Data for this study were prepared, archived, and distributed by the National Institute on Aging Alzheimer's Disease Data Storage Site (NIAGADS) at the University of Pennsylvania (U24-AG041689-01); Alzheimer's Disease Genetics Consortium (ADGC), U01 AG032984, RC2 AG036528; NACC, U01 AG016976; NIA-LOAD (Columbia University), U24 AG026395, U24 AG026390, R01AG041797; Banner Sun Health Research Institute P30 AG019610; Boston University, P30 AG013846, U01 AG10483, R01 CA129769, R01 MH080295, R01 AG017173, R01 AG025259, R01 AG048927, R01AG33193, R01 AG009029; Columbia University, P50 AG008702, R37 AG015473, R01 AG037212, R01 AG028786; Duke University, P30 AG028377, AG05128; Group Health Research Institute, UO1 AG006781, UO1 HG004610, UO1 HG006375, UO1 HG008657; Indiana University, P30 AG10133, R01 AG009956, RC2 AG036650; Johns Hopkins University, P50 AG005146, R01 AG020688; Massachusetts General Hospital, P50 AG005134; Mayo Clinic, P50 AG016574, R01 AG032990, KL2 RR024151; Mount Sinai School of Medicine, P50 AG005138, P01 AG002219; New York University, P30 AG08051, UL1 RR029893, 5R01AG012101, 5R01AG022374, 5R01AG013616, 1RC2AG036502, 1R01AG035137; Northwestern University, P30 AG013854; Oregon Health & Science University, P30 AG008017, R01 AG026916; Rush University, P30 AG010161, R01 AG019085, R01 AG15819, R01 AG17917, R01 AG030146, R01 AG01101, RC2 AG036650, R01 AG22018; TGEN, R01 NS059873; University of Alabama at Birmingham, P50 AG016582, UL1RR02777; University of Arizona, R01 AG031581; University of California, Davis, P30 AG010129; University of California, Irvine, P50 AG016573, P50 AG016575, P50 AG016576, P50 AG016577; University of California, Los Angeles, P50 AG016570; University of California, San Diego, P50 AG005131; University of California, San Francisco, P50 AG023501, P01 AG019724; University of Kentucky, P30 AG028383, AG05144; University of Michigan, P30 AG053760 and AG063760; University of Pennsylvania, P30 AG010124; University of Pittsburgh, P50 AG005133, AG030653, AG041718, AG07562, AG02365; University of Southern California, P50 AG005142; University of Texas Southwestern, P30 AG012300; University of Miami, R01 AG027944, AG010491, AG027944, AG021547, AG019757; University of Washington, P50 AG005136, R01 AG042437; University of Wisconsin, P50 AG033514; Vanderbilt University, R01 AG019085; and Washington University, P50 AG005681, P01 AG03991, P01 AG026276. The Kathleen Price Bryan Brain Bank at Duke University Medical Center is funded by NINDS grant # NS39764, NIMH MH60451 and by Glaxo Smith Kline. Genotyping of the TGEN2 cohort was supported by Kronos Science. The TGen series was also funded by NIA grant AG041232, The Banner Alzheimer's Foundation, The Johnnie B. Byrd Sr. Alzheimer's Institute, the Medical Research Council, and the state of Arizona and also includes samples from the following sites: Newcastle Brain Tissue Resource (funding via the Medical Research Council, local NHS trusts and Newcastle University), MRC London Brain Bank for Neurodegenerative



Diseases (funding via the Medical Research Council), South West Dementia Brain Bank (funding via numerous sources including the Higher Education Funding Council for England (HEFCE), Alzheimer's Research Trust (ART), BRACE as well as North Bristol NHS Trust Research and Innovation 58 Department and DeNDRoN), The Netherlands Brain Bank (funding via numerous sources including Stichting MS Research, Brain Net Europe, Hersenstichting Nederland Breinbrekend Werk, International Parkinson Fonds, Internationale Stichting Alzheimer Onderzoek), Institut de Neuropatologia, Servei Anatomia Patologica, Universitat de Barcelona. The NACC database is funded by NIA/NIH Grant U01 AG016976. NACC data are contributed by the NIA-funded ADCs: P30 AG019610 (PI Eric Reiman, MD), P30 AG013846 (PI Neil Kowall, MD), P30 AG062428-01 (PI James Leverenz, MD) P50 AG008702 (PI Scott Small, MD), P50 AG025688 (PI Allan Levey, MD, PhD), P50 AG047266 (PI Todd Golde, MD, PhD), P30 AG010133 (PI Andrew Saykin, PsyD), P50 AG005146 (PI Marilyn Albert, PhD), P30 AG062421-01 (PI Bradley Hyman, MD, PhD), P30 AG062422-01 (PI Ronald Petersen, MD, PhD), P50 AG005138 (PI Mary Sano, PhD), P30 AG008051 (PI Thomas Wisniewski, MD), P30 AG013854 (PI Robert Vassar, PhD), P30 AG008017 (PI Jeffrey Kaye, MD), P30 AG010161 (PI David Bennett, MD), P50 AG047366 (PI Victor Henderson, MD, MS), P30 AG010129 (PI Charles DeCarli, MD), P50 AG016573 (PI Frank LaFerla, PhD), P30 AG062429-01 (PI James Brewer, MD, PhD), P50 AG023501 (PI Bruce Miller, MD), P30 AG035982 (PI Russell Swerdlow, MD), P30 AG028383 (PI Linda Van Eldik, PhD), P30 AG053760 (PI Henry Paulson, MD, PhD), P30 AG010124 (PI John Trojanowski, MD, PhD), P50 AG005133 (PI Oscar Lopez, MD), P50 AG005142 (PI Helena Chui, MD), P30 AG012300 (PI Roger Rosenberg, MD), P30 AG049638 (PI Suzanne Craft, PhD), P50 AG005136 (PI Thomas Grabowski, MD), P30 AG062715-01 (PI Sanjay Asthana, MD, FRCP), P50 AG005681 (PI John Morris, MD), P50 AG047270 (PI Stephen Strittmatter, MD, PhD). The genotypic and associated phenotypic data used in the study "Multi-Site Collaborative Study for Genotype-Phenotype Associations in Alzheimer's Disease (GenADA)" were provided by the GlaxoSmithKline, R&D Limited. ROSMAP study data were provided by the Rush Alzheimer's Disease Center, Rush University Medical Center, Chicago. Data collection was supported through funding by NIA grants P30AG10161, R01AG15819, R01AG17917, R01AG30146, R01AG36836, U01AG32984, U01AG46152, the Illinois Department of Public Health, and the Translational Genomics Research Institute. The AddNeuroMed data are from a public-private partnership supported by EFPIA companies and SMEs as part of InnoMed (Innovative Medicines in Europe), an Integrated Project funded by the European Union of the Sixth Framework program priority FP6-2004-LIFESCIHEALTH-5. Clinical leads responsible for data collection are Iwona Kłoszewska (Lodz), Simon Lovestone (London), Patrizia Mecocci (Perugia), Hilikka Soininen (Kuopio), Magda Tsolaki (Thessaloniki), and Bruno Vellas (Toulouse), imaging leads are Andy Simmons (London), Lars-Olad Wahlund (Stockholm) and Christian Spenger (Zurich) and bioinformatics leads are Richard Dobson (London) and Stephen Newhouse (London). Data collection and

sharing for this project was funded by the Alzheimer's Disease Neuroimaging Initiative (ADNI) (National Institutes of Health Grant U01 AG024904) and DOD ADNI (Department of Defense award number W81XWH-12-2-0012). ADNI is funded by the National Institute on Aging, the National Institute of Biomedical Imaging and Bioengineering and through generous contributions from the following: AbbVie. Alzheimer's Association; Alzheimer's Drug Discovery Foundation; Araclon Biotech; BioClinica. Inc.; Biogen; Bristol-Myers Squibb Company; CereSpir. Inc.; Cogstate; Eisai Inc.; Elan Pharmaceuticals. Inc.; Eli Lilly and Company; EuroImmun; F. Hoffmann-La Roche Ltd and its affiliated company Genentech. Inc.; Fujirebio; GE HealthControlsare; IXICO Ltd.; Janssen Alzheimer Immunotherapy Research & Development. LLC.; Johnson & Johnson Pharmaceutical Research & Development LLC.; Lumosity; Lundbeck; Merck & Co. Inc.; Meso Scale Diagnostics. LLC.; NeuroRx Research; Neurotrack Technologies; Novartis Pharmaceuticals Corporation; Pfizer Inc.; Piramal Imaging; Servier; Takeda Pharmaceutical Company; and Transition Therapeutics. The Canadian Institutes of Health Research is providing funds to support ADNI clinical sites in Canada. Private sector contributions are facilitated by the Foundation for the National Institutes of Health. The grantee organization is the Northern California Institute for Research and Education, and the study is coordinated by the Alzheimer's Therapeutic Research Institute at the University of Southern California. ADNI data are disseminated by the Laboratory for Neuro Imaging at the University of Southern California. The authors thank the Clinical and Genetics Cores of the Knight ADRC at Washington University for clinical and cognitive assessments of the participants and for APOE genotypes (Charles and Joanne Knight Alzheimer's Research Initiative of the Washington University Alzheimer's Disease Research Centre) and the Biomarker Core of the Adult Children Study at Washington University for the CSF collection and assays (Recruitment and CSF studies at University of Washington were supported by NIH PO1 AGO5131).

## CONFLICT OF INTEREST STATEMENT

The authors declare no competing interests.

## DATA AVAILABILITY STATEMENT

Data sharing is not applicable to this article as no new data were created or analyzed in this study.

## ORCID

Serena Dato <https://orcid.org/0000-0003-2589-7929>

Francesco De Rango <https://orcid.org/0000-0002-2328-8487>

Paolina Crocco <https://orcid.org/0000-0001-7803-5340>

Stefano Pallotti <https://orcid.org/0000-0003-3196-151X>

Michael E. Belloy <https://orcid.org/0000-0001-7748-9033>

Yann Le Guen <https://orcid.org/0000-0001-6649-8364>

Michael D. Greicius <https://orcid.org/0000-0002-5462-9037>

Giuseppe Passarino <https://orcid.org/0000-0003-4701-9748>

Giuseppina Rose <https://orcid.org/0000-0002-4264-4184>

Valerio Napolioni <https://orcid.org/0000-0002-4378-6838>



## REFERENCES

- 1000 Genomes Project Consortium, Auton, A., Brooks, L. D., Durbin, R. M., Garrison, E. P., Kang, H. M., Korbel, J. O., Marchini, J. L., McCarthy, S., McVean, G. A., & Abecasis, G. R. (2015). A global reference for human genetic variation. *Nature*, 526(7571), 68–74. <https://doi.org/10.1038/nature15393>
- Abondio, P., Sazzini, M., Garagnani, P., Boattini, A., Monti, D., Franceschi, C., Luiselli, D., & Giuliani, C. (2019). The Genetic variability of APOE in different human populations and its implications for longevity. *Genes*, 10(3), 222. <https://doi.org/10.3390/genes10030222>
- Akhtar, A., & Sah, S. P. (2020). Insulin signaling pathway and related molecules: Role in neurodegeneration and Alzheimer's disease. *Neurochemistry International*, 135, 104707. <https://doi.org/10.1016/j.neuint.2020.104707>
- Akiyama, H., Barger, S., Barnum, S., Bradt, B., Bauer, J., Cole, G. M., Cooper, N. R., Eikelenboom, P., Emmerling, M., Fiebich, B. L., Finch, C. E., Frautschy, S., Griffin, W. S., Hampel, H., Hull, M., Landreth, G., Lue, L., Mrak, R., Mackenzie, I. R., ... Wyss-Coray, T. (2000). Inflammation and Alzheimer's disease. *Neurobiology of Aging*, 21(3), 383–421. [https://doi.org/10.1016/s0197-4580\(00\)00124-x](https://doi.org/10.1016/s0197-4580(00)00124-x)
- Andrews, S. J., Renton, A. E., Fulton-Howard, B., Podlesny-Drabiniok, A., Marcora, E., & Goate, A. M. (2023). The complex genetic architecture of Alzheimer's disease: Novel insights and future directions. *eBioMedicine*, 90, 104511. <https://doi.org/10.1016/j.ebiom.2023.104511>
- Bacalini, M., Palombo, F., Garagnani, P., Giuliani, C., Fiorini, C., Caporali, L., Stanzani Maserati, M., Capellari, S., Romagnoli, M., De Fanti, S., Benussi, L., Binetti, G., Ghidoni, R., Galimberti, D., Scarpini, E., Arcaro, M., Bonanni, E., Siciliano, G., Maestri, M., ... Santoro, A. (2022). Association of rs3027178 polymorphism in the circadian clock gene PER1 with susceptibility to Alzheimer's disease and longevity in an Italian population. *GeroScience*, 44, 881–896. <https://doi.org/10.1007/s11357-021-00477-0>
- Barbieri, M., Bonafè, M., Franceschi, C., & Paolisso, G. (2003). Insulin/IGF-I-signaling pathway: An evolutionarily conserved mechanism of longevity from yeast to humans. *American Journal of Physiology. Endocrinology and Metabolism*, 285(5), E1064–E1071. <https://doi.org/10.1152/ajpendo.00296.2003>
- Behl, C. (2000). Apoptosis and Alzheimer's disease. *Journal of Neural Transmission (Vienna)*, 107(11), 1325–1344. <https://doi.org/10.1007/s007020070021>
- Chang, C. C., Chow, C. C., Tellier, L. C., Vattikuti, S., Purcell, S. M., & Lee, J. J. (2015). Second-generation PLINK: Rising to the challenge of larger and richer datasets. *Gigascience*, 4, 7. <https://doi.org/10.1186/s13742-015-0047-8>
- Chen, C. Y., Pollack, S., Hunter, D. J., Hirshhorn, J. N., Kraft, P., & Price, A. L. (2013). Improved ancestry inference using weights from external reference panels. *Bioinformatics*, 29, 1399–1406. <https://doi.org/10.1093/bioinformatics/btt144>
- Das, S., Forer, L., Schönerr, S., Sidore, C., Locke, A. E., Kwong, A., Vrieze, S. I., Chew, E. Y., Levy, S., McGue, M., Schlessinger, D., Stambolian, D., Loh, P. R., Iacono, W. G., Swaroop, A., Scott, L. J., Cucca, F., Kronenberg, F., Boehnke, M., ... Fuchsberger, C. (2016). Next-generation genotype imputation service and methods. *Nature Genetics*, 48, 1284–1287. <https://doi.org/10.1038/ng.3656>
- Dato, S., Crocco, P., De Rango, F., Iannone, F., Maletta, R., Bruni, A. C., Saiardi, A., Rose, G., & Passarino, G. (2021). IP6K3 and IPMK variations in LOAD and longevity: Evidence for a multifaceted signaling network at the crossroad between neurodegeneration and survival. *Mechanisms of Ageing and Development*, 195, 111439. <https://doi.org/10.1016/j.mad.2021.111439>
- Dato, S., Soerensen, M., De Rango, F., Rose, G., Christensen, K., Christiansen, L., & Passarino, G. (2018). The genetic component of human longevity: New insights from the analysis of pathway-based SNP-SNP interactions. *Aging Cell*, 17(3), e12755. <https://doi.org/10.1111/ace1.12755>
- de la Monte, S. M., & Wands, J. R. (2005). Review of insulin and insulin-like growth factor expression, signaling, and malfunction in the central nervous system: Relevance to Alzheimer's disease. *Journal of Alzheimer's Disease*, 7(1), 45–61. <https://doi.org/10.3233/jad-2005-7106>
- Deelen, J., Evans, D. S., Arking, D. E., Tesi, N., Nygaard, M., Liu, X., Wojczynski, M. K., Biggs, M. L., van der Spek, A., Atzmon, G., Ware, E. B., Sarnowski, C., Smith, A. V., Seppälä, I., Cordell, H. J., Dose, J., Amin, N., Arnold, A. M., Ayers, K. L., ... Murabito, J. M. (2019). A meta-analysis of genome-wide association studies identifies multiple longevity genes. *Nature Communications*, 10(1), 3669. <https://doi.org/10.1038/s41467-019-11558-2>
- Fan, C. C., Banks, S. J., Thompson, W. K., Chen, C. H., McEvoy, L. K., Tan, C. H., Kukull, W., Bennett, D. A., Farrer, L. A., Mayeux, R., Schellenberg, G. D., Andreassen, O. A., Desikan, R., & Dale, A. M. (2020). Sex-dependent autosomal effects on clinical progression of Alzheimer's disease. *Brain*, 143(7), 2272–2280. <https://doi.org/10.1093/brain/awaa164>
- Gilbert-Diamond, D., & Moore, J. H. (2011). Analysis of gene-gene interactions. *Current Protocols in Human Genetics*, 1, 14. <https://doi.org/10.1002/0471142905.hg0114s70>
- Gui, H., Gong, Q., Jiang, J., Liu, M., & Li, H. (2021). Identification of the hub genes in Alzheimer's Disease. *Computational and Mathematical Methods in Medicine*, 2021, 6329041. <https://doi.org/10.1155/2021/6329041>
- Hivert, V., Sidorenko, J., Rohart, F., Goddard, M. E., Yang, J., Wray, N. R., Yengo, L., & Visscher, P. M. (2021). Estimation of non-additive genetic variance in human complex traits from a large sample of unrelated individuals. *American Journal of Human Genetics*, 108(5), 786–798. <https://doi.org/10.1016/j.ajhg.2021.02.014>
- Hossin, M. Z. (2021). The male disadvantage in life expectancy: Can we close the gender gap? *International Health*, 13(5), 482–484. <https://doi.org/10.1093/inthealth/ihaa106>
- Iannuzzi, V., Bacalini, M. G., Franceschi, C., & Giuliani, C. (2023). The role of genetics and epigenetics in sex differences in human survival. *Genus*, 79, 1. <https://doi.org/10.1186/s41118-023-00181-1>
- Iatrou, A., Clark, E. M., & Wang, Y. (2021). Nuclear dynamics and stress responses in Alzheimer's disease. *Molecular Neurodegeneration*, 16(1), 65. <https://doi.org/10.1186/s13024-021-00489-6>
- Ihara, Y., Hayabara, T., Sasaki, K., Kawada, R., Nakashima, Y., & Kuroda, S. (2000). Relationship between oxidative stress and apoE phenotype in Alzheimer's disease. *Acta Neurologica Scandinavica*, 102(6), 346–349. <https://doi.org/10.1034/j.1600-0404.2000.102006346.x>
- Jagust, W. (2018). Imaging the evolution and pathophysiology of Alzheimer disease. *Nature Reviews Neuroscience*, 19(11), 687–700. <https://doi.org/10.1038/s41583-018-0067-3>
- Kuningas, M., Mooijaart, S. P., van Heemst, D., Zwaan, B. J., Slagboom, P. E., & Westendorp, R. G. (2008). Genes encoding longevity: From model organisms to humans. *Aging Cell*, 7, 270–280. <https://doi.org/10.1111/j.1474-9726.2008.00366.x>
- Kwong, J. Q., Beal, M. F., & Manfredi, G. (2006). The role of mitochondria in inherited neurodegenerative diseases. *Journal of Neurochemistry*, 97(6), 1659–1675. <https://doi.org/10.1111/j.1471-4159.2006.03990.x>
- Lagou, V., Mägi, R., Hottenga, J.-J., Grallert, H., Perry, J. R. B., Bouatia-Naji, N., Marullo, L., Rybin, D., Jansen, R., Min, J. L., Dimas, A. S., Ulrich, A., Zudina, L., Gädin, J. R., Jiang, L., Faggian, A., Bonnefond, A., Fadista, J., Stathopoulou, M. G., ... Meta-Analyses of Glucose and Insulin-related traits Consortium (MAGIC). (2021). Sex-dimorphic genetic effects and novel loci for fasting glucose and insulin variability. *Nature Communications*, 12(1), 24. <https://doi.org/10.1038/s41467-020-19366-9>
- Leclerc, M., Bourassa, P., Tremblay, C., Caron, V., Sugère, C., Emond, V., Bennett, D. A., & Calon, F. (2023). Cerebrovascular insulin receptors



- are defective in Alzheimer's disease. *Brain*, 146(1), 75–90. <https://doi.org/10.1093/brain/awac309>
- Long, J. M., & Holtzman, D. M. (2019). Alzheimer Disease: An update on pathobiology and treatment strategies. *Cell*, 179(2), 312–339. <https://doi.org/10.1016/j.cell.2019.09.001>
- Machiela, M. J., & Chanock, S. J. (2015). LDlink: A web-based application for exploring population-specific haplotype structure and linking correlated alleles of possible functional variants. *Bioinformatics*, 31, 3555–3557. <https://doi.org/10.1093/bioinformatics/btv402>
- Mägi, R., & Morris, A. P. (2010). GWAMA: Software for genome-wide association meta-analysis. *BMC Bioinformatics*, 11, 288. <https://doi.org/10.1186/1471-2105-11-288>
- Misawa, T., Arima, K., Mizusawa, H., & Satoh, J. (2008). Close association of water channel AQP1 with amyloid-beta deposition in Alzheimer disease brains. *Acta Neuropathologica*, 116(3), 247–260. <https://doi.org/10.1007/s00401-008-0387-x>
- Mishra, A., & Macgregor, S. (2015). VEGAS2: Software for more flexible gene-based testing. *Twin Research and Human Genetics*, 18(1), 86–91. <https://doi.org/10.1017/thg.2014.79>
- Napolioni, V., Scelsi, M. A., Khan, R. R., Altmann, A., & Greicius, M. D. (2021). Recent consanguinity and outbred Autozygosity are associated with increased risk of late-onset Alzheimer's Disease. *Frontiers in Genetics*, 11, 629373. <https://doi.org/10.3389/fgene.2020.629373>
- Nebel, R. A., Aggarwal, N. T., Barnes, L. L., Gallagher, A., Goldstein, J. M., Kantarci, K., Mallampalli, M. P., Mormino, E. C., Scott, L., Yu, W. H., Maki, P. M., & Mielke, M. M. (2018). Understanding the impact of sex and gender in Alzheimer's disease: A call to action. *Alzheimer's & Dementia*, 14(9), 1171–1183. <https://doi.org/10.1016/j.jalz.2018.04.008>
- Ridge, P. G., Hoyt, K. B., Boehme, K., Mukherjee, S., Crane, P. K., Haines, J. L., Mayeux, R., Farrer, L. A., Pericak-Vance, M. A., Schellenberg, G. D., Kauwe, J. S. K., & Alzheimer's Disease Genetics Consortium (ADGC). (2016). Assessment of the genetic variance of late-onset Alzheimer's disease. *Neurobiology of Aging*, 41, 200.e13–200.e20. <https://doi.org/10.1016/j.neurobiolaging.2016.02.024>
- Riedel, B. C., Thompson, P. M., & Brinton, R. D. (2016). Age, APOE and sex: Triad of risk of Alzheimer's disease. *The Journal of Steroid Biochemistry and Molecular Biology*, 160, 134–147. <https://doi.org/10.1016/j.jsbmb.2016.03.012>
- Ritchie, M. D., Hahn, L. W., Roodi, N., Bailey, L. R., Dupont, W. D., Parl, F. F., & Moore, J. H. (2001). Multifactor-dimensionality reduction reveals high-order interactions among estrogen-metabolism genes in sporadic breast cancer. *American Journal of Human Genetics*, 69(1), 138–147. <https://doi.org/10.1086/321276>
- Singhal, P., Verma, S. S., & Ritchie, M. D. (2023). Gene interactions in human disease studies-evidence is mounting. *Annual Review of Biomedical Data Science*, 6, 377–395. <https://doi.org/10.1146/annurev-biodatasci-102022-120818>
- Tesi, N., Hulsman, M., van der Lee, S. J., Jansen, I. E., Stringa, N., van Schoor, N. M., Scheltens, P., van der Flier, W. M., Huisman, M., Reinders, M. J. T., & Holstege, H. (2021). The effect of Alzheimer's Disease-associated Genetic variants on longevity. *Frontiers in Genetics*, 12, 748781. <https://doi.org/10.3389/fgene.2021.748781>
- Ukrainseva, S., Duan, M., Arbeeve, K., Wu, D., Bagley, O., Yashkin, A. P., Gorbunova, G., Akushevich, I., Kulminski, A., & Yashin, A. (2021). Interactions between genes from aging pathways may influence human lifespan and improve animal to human translation. *Frontiers in Cell and Development Biology*, 9, 692020. <https://doi.org/10.3389/fcell.2021.692020>
- Yan, Y., Dominguez, S., Fisher, D. W., & Dong, H. (2018). Sex differences in chronic stress responses and Alzheimer's disease. *Neurobiology of Stress*, 8, 120–126. <https://doi.org/10.1016/j.ynstr.2018.03.002>
- Young, A. L., Marinescu, R. V., Oxtoby, N. P., Bocchetta, M., Yong, K., Firth, N. C., Cash, D. M., Thomas, D. L., Dick, K. M., Cardoso, J., van Swieten, J., Borroni, B., Galimberti, D., Masellis, M., Tartaglia, M. C., Rowe, J. B., Graff, C., Tagliavini, F., Frisoni, G. B., ... Genetic FTD Initiative (GENFI) & Alzheimer's Disease Neuroimaging Initiative (ADNI). (2018). Uncovering the heterogeneity and temporal complexity of neurodegenerative diseases with subtype and stage inference. *Nature Communications*, 9, 4273. <https://doi.org/10.1038/s41467-018-05892-0>
- Zeng, Y., Nie, C., Min, J., Chen, H., Liu, X., Ye, R., Chen, Z., Bai, C., Xie, E., Yin, Z., Lv, Y., Lu, J., Li, J., Ni, T., Bolund, L., Land, K. C., Yashin, A., O'Rand, A. M., Sun, L., ... Vaupel, J. (2018). Sex differences in Genetic associations with longevity. *JAMA Network Open*, 1(4), e181670. <https://doi.org/10.1001/jamanetworkopen.2018.1670>
- Zhang, L., Young, J. I., Gomez, L., Silva, T. C., Schmidt, M. A., Cai, J., Chen, X., Martin, E. R., & Wang, L. (2021). Sex-specific DNA methylation differences in Alzheimer's disease pathology. *Acta Neuropathologica Communications*, 9(1), 77. <https://doi.org/10.1186/s40478-021-01177-8>

## SUPPORTING INFORMATION

Additional supporting information can be found online in the Supporting Information section at the end of this article.

**How to cite this article:** Dato, S., De Rango, F., Crocco, P., Pallotti, S., Belloy, M. E., Le Guen, Y., Greicius, M. D., Passarino, G., Rose, G., & Napolioni, V. (2023). Sex- and APOE-specific genetic risk factors for late-onset Alzheimer's disease: Evidence from gene-gene interaction of longevity-related loci. *Aging Cell*, 22, e13938. <https://doi.org/10.1111/ace1.13938>